Mechanics of Advanced Composite Structures

Journal homepage: https://macs.semnan.ac.ir/

Semnan University

ISSN: 2423-7043

Research Article

Reinforced Concrete Two-Way Slabs Exposed to Impulse Loadings

Ola Mazen Makki

Department of Civil Engineering, College of Engineering, University of Al-Qadisiyah, Al-Qadisiyah, Iraq

ARTICLE INFO

Article history:

Received: 2024-10-19
Revised: 2025-03-22
Accepted: 2025-05-12

Keywords:

Impulse load;
Dynamic loads,
Two-way slab;
Reinforced concrete slab;
Free vibrations.

ABSTRACT

Concrete two-way slabs could be subjected to impulse load due to accidents, which force the structural member to undergo strain hardening faster than its ability to dampen and absorb much of the applied energy, which has not been previously investigated in the literature. Theoretical and numerical models were developed and validated against experimental results to explore this behavior. A reinforced concrete square slab of 1 m length and 0.08m thickness was simulated with several case studies investigated, such as the impulse load intensity, concrete compressive strength magnitude, the model's free vibration, and the model solution. It was concluded that the slab's response under impulse load depends, to the first degree, on the impulse quantity. If this sudden load equals two-thirds of the static load, the model starts to show visible cracks. Furthermore, the maximum displacement does not necessarily occur at the instant of loading; unlike static conditions, the designer can expect the higher deflection several seconds after the applied load is applied.

1. Introduction

Constructions are exposed to several dynamic loads (as a time-dependent force) besides the monotonic loads during their service life. Dynamic loads generally accelerate the member and activate its velocity, which affects the member mass and the damping factor. There are many dynamic loads, such as impact, impulse, cyclic, harmonic, transient, and seismic loads. Impulsive or shock loads are frequently significant in designing specific structural systems, e.g., vehicles such as trucks, automobiles, or traveling cranes. [1]. An impulse load is a short-duration, very high intensity of a stepped load that is applied for a very short period. This type of dynamic load, as well as all extra types of dynamic loads, causes a high rate of straining and attacks the mass, damping, and stiffness of the member, which leads to strain hardening for the material. The damping factor is of little importance in controlling the maximum response of members exposed to impulse load because the maximum response to a particular impulsive load will be reached quickly. [1], [2].

Stain hardening happens when a significant and fast load is applied for a short period of time; at that moment, the stressed material particles cannot deform and redistribute under such fast stress, so it fails suddenly. Most metals, especially steel, tend to exhibit enhanced mechanical properties at high strain rates due to dynamic loads compared to their properties under static and quasi-static loading. This phenomenon occurs when exposed to high rates of dynamic loadings or even high rates of monotonic loads.

* **Corresponding author.**
E-mail address: Ola.Mazen@qu.edu.iq

Cite this article as:
Mohammadi, A. and Mahdi-Nia, M., 2026. Title of article. *Mechanics of Advanced Composite Structures*, 13(1), pp. xxx-xxx.
https://doi.org/10.22075/MACS.2025.39315.2050

The reinforced concrete two-way slab was discussed widely in different materials and additives besides the conventional concrete under monotonic loads. [3], [4], Cyclic loads [5], harmonic loads [6], [7], and impact loads [8], [9], [10]. Too few articles in the literature deal with the impulse load besides the two-way reinforced concrete slabs under pulse load. The Shape memory alloy (SMA) hybrid composite beams were investigated under the exposure of impulse load, considering the instantaneous phase transformation. [11]. Based on the reference results, as the amplitude of the impulse loading rises, the SMA wires display a greater ability to dampen the response amplitude. In other words, the SMA wires behave as a useful innovative material for vibration damping in construction applications, so the dissolution of vibration response is viewed significantly more quickly.

Miyamoto et al.[12] introduced an analytical model for the reinforced concrete slab subjected to an impulse load. The theoretical solution agreed with the actual phenomenon and found that the failure patterns are influenced by the loading values and impulse from the impulsive load equation.

The influence of applying a pulse load during the construction of concrete slabs was investigated previously by Muttashar M.[13]It was found that significant damage was observed between the seconds 91-97 sec, while the overall load period reached 398 sec. Besides, to treat the building construction exposed to impulse load, a longitudinal reinforcement near the neutral axis could be placed to treat the slab member. [13].

Zahid M.A.[14] investigated experimentally and theoretically the effect of the impact load on cambered reactive powder concrete slabs using the falling mass method. The maximum and minimum kinematic energy used were 93 Joules and 17 Joule respectively. Many parameters were investigated, such as steel fiber amount, main reinforcement ratio, slab thickness, and loading plate stiffness. It was concluded that by creating a cambering up to (20 mm), the maximum mid-span displacement, permanent deflection, and crack width are decreased by about 65%, 86%, 67% respectively. Ultrasonic Pulse Velocity (UPV) test showed that cambering of (10 mm) has reduced the visible cracks' width but multiplied the number of invisible cracks, whereas a cambered slab (20 mm) has minimized both the visible crack's width and the number of invisible cracks.

Hrynyk T. [15] Seven slabs of intermediate size were built and put through a failure test under successive drop-weight impacts. In addition to having longitudinal reinforcing bars, the slabs were built with steel fiber concentrations that ranged from zero (traditional reinforced concrete) to 1.50 percent by volume. The testing program's data were utilized to further evaluate steel fiber-reinforced concretes' performance in impact-resistant applications and to offer a well-documented dataset related to a field of study that is currently underrepresented in the literature. The test findings demonstrated that the steel fiber addition effectively increased slab capacity, decreased fracture widths and spacings, and mitigated local impact damage.

Concrete, as a material, is brittle in normal cases and can convert its behavior into ductile by using some additives. Steel fibers, wherever their type was working on gaining the concrete some ductility by enhancing all the mechanical properties of the material, and working on merging the crack sides to delay the failure [16], [17], [18], [19]. Also, replacing a percentage of aggregate (gravel or sand or both) with the same size and grades of scraped ties rubbers also modified the concrete ductility. [20], [21], [22]. The rubbers inside the concrete mix (which is considered a new material called rubcrete) work as micro-embedded springs inside the concrete particles, leading to a greater resistance against the dynamic loadings, despite its mechanical properties being lower than those of conventional concrete [21]. Because of that, the rubber has an elastic modulus that differs widely from the other concrete component's young modulus, and that difference creates several microcracks between the cement paste and rubber particles. [20], [21], [23]. So this article focuses on studying the behavior of conventional concrete two-way slabs, steel fibered concrete slabs, rubcrete slabs, and slabs containing both steel fibers and rubber under several cases of dynamic loadings.

2. Investigation Methodology

The monotonically tested reactive powder concrete two-way slab, which was tested experimentally within the reference [3], was used to verify the numerical analysis of this article. The slab of dimensions equal $1000 \times 1000 \times 80\ mm$ was solved using yield line theory under the effect of monotonic (static) loads to evaluate the estimated collapse load of the model. Then, these experimental and theoretical solutions were used to clarify the numerical model. Numerical analysis using ANSYS APDL (Version 2019) was first made as a static load to compare with the failure load, estimated from the theory, and the same slab dimensions were utilized to investigate the effect of pulse load on the slab. Six rebars in each direction were utilized with a yielding and fracture stress equal to 475 MPa and 523 MPa, respectively.

An impulse load was subjected to a point load similar to the theoretical solution of the static load with different amounts of impulse and over 0.1 sec (as shown in Fig. 1). It is essential to mention that the shape of the pulse is rectangular. The study investigates the effect of load intensity on the slab, the compressive strength of the concrete, and the change in the concrete material to rubberized concrete.

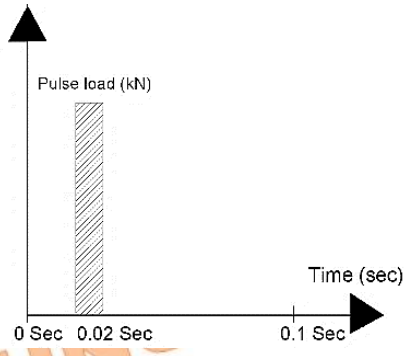

Fig. 1. Applied impulse load diagram

3. Theoretical Solution by Yield Line Theory

Two methods of analyzing structural members could be used to estimate the failure collapse load for the members: lower- and upper-bound theories. [24], [25]. The lower bound theory gives the collapse load just before starting to yield. Meanwhile, the upper bound theory gives an ultimate correct or higher load than the actual value. So, the upper bound theory was used in this study to approve and certify the numerical analysis. The failure mechanism and the calculation details are illustrated in Fig. 2.

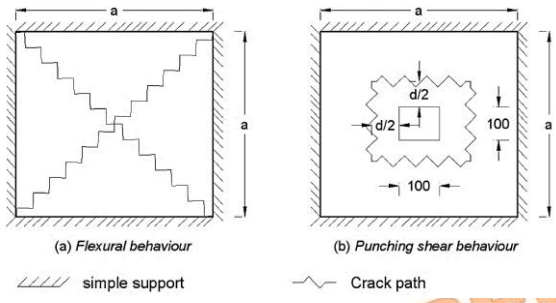

Fig. 2. The expected yield line crack patterns and slab failure modes

3.1. Bending strength solutions

$$As\ of\ one\ bar = 28.286\ mm^2 \quad (1)$$

$$As\ in\ whole\ member = 188.57\ mm^2 \quad (2)$$

$$0.00159 > \rho = 0.00281 \quad (3)$$

$$a = \frac{As\ fy}{0.85\ f'c\ b} = 1.35\ mm \quad (4)$$

$$a = \frac{As\ fy}{0.85\ f'c\ b} = 1.35\ mm \quad (5)$$

$$M_n = As\ fy\ \left(d - \frac{a}{2}\right) = 5.94\ kN.m \quad (6)$$

$$\text{External work} = P\ \delta, \quad \text{while internal work} = m\ a \quad (7)$$

$$\text{Internal work} = m^+ \times a \times \frac{\delta}{0.5a} = 2m^+\delta \quad (8)$$

$$\sum internal\ work = 4 \times 2 \times m^+ \times \delta = 8m^+\delta \quad (9)$$

When equating between internal and external work, got:

$$8m^+\delta = P\ \delta \Rightarrow p = 8m^+ \Rightarrow P = 8 \times 5.94 = 47.52\ kN \quad (10)$$

3.2. Shear strength calculations

$$V_c = \frac{1}{3}\sqrt{f'c} \times b_\circ \times \frac{d}{1000} \quad (11)$$

$$b_\circ = 4(100 + d) = 668\ mm \quad (12)$$

$$v_c = 131.75\ kN > p = 47.52kN \quad (13)$$

which means that the slab failed by bending before punching shear occurs.

4. Numerical Inputs and Analysis

Solid 65 (a hexahedral brick element) was selected for simulating concrete material. It is an eighty-node isoperimetric brick element; each node contains three degrees of freedom (DOF): u in the x coordinate, v in the y axis, and w in the z coordinate. Solid 65 is suitable for representing concrete due to its ability to crack in 3-direction orthogonally, its creeping and crushing behavior, and finally, its capability to deform plastically. Solid 65 is defined as a linear behavior (inserting Young's modulus and Poisson's ratio) and a nonlinear behavior by specifying the stress versus strain curve, concrete properties, and concrete mass [26], [27].

Link180 is a truss element, a uniaxial tension-compression element of three degrees of freedom at each node. It includes significant properties like creep, plasticity, stress stiffening, swelling, and large deformation capacity. It's defined by linear and bilinear behavior to view the steel plasticity [28].

The SOLID185 element was suitable for use in steel-bearing plate material. The element has eight nodes with three degrees of freedom at each

one of its nodes' translations in the nodal x, y, and z directions. The element was defined only by elastic modulus and Poisson's ratio to keep it within the elastic range and avoid absorbing the applied load [29], [30].

Simply supporting was selected at all slab edges, and the analysis was done using a modified Newton-Raphson method with a tolerance of 0.001. The model before analysis, steel rebars, and meshing are shown in Fig. 3.

Modeling rubberized concrete could be provided in ANSYS APDL using the rubcrete elastic modulus, stress-strain curves for the mixes, and the rubcrete tensile and compressive strengths. Three stress vs. strain curves for the rubberized concrete (S10, S20, and S30) were selected to be simulated with the program published at the reference [31].

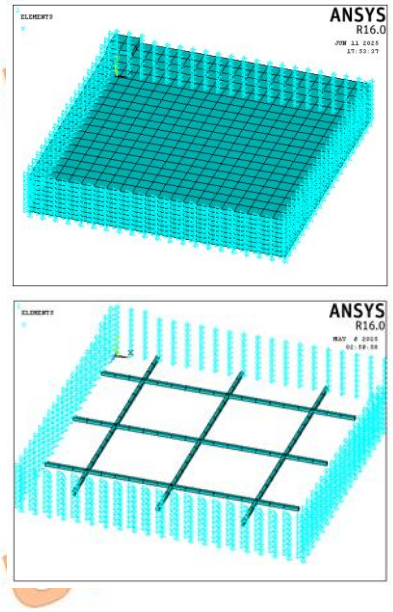

Fig.3. Meshed concrete and steel elements with support and axes of symmetry

5. Results And Discussions

5.1. Verify The Model

Several mesh sizes were used to find a solution matching the yield line theory and the experimental results, which were published in reference [3]. The numerical model, after analysis, failed at exactly 46.2 kN. This little difference could be due to the more realistic model of nature, which considers all the details of concrete, from cracking, creeping, and shrinking, compared with the theoretical solution. The load deflection curves for the numerical and experimental models are listed in Fig. 4. It can be concluded that the slab begins with the elastic behaviour till 20 kN, then it undergoes the nonlinearity up to the failure at 46 kN. The numerical deflection is slightly less than the experiment; due to that, the numerical models in general do not contain plastic shrinkage cracks and the initial formation of microcracks.

5.2. Modal Analysis

The primary foundation for all dynamic analysis and its starting point is the model analysis due to many reasons, such as examination of the modes of failure of the specimen, calculating the period of vibration, and finding the natural frequencies of all modes of failure to avoid the interaction with the frequencies of applied load, in which the structure may continue to resonate then damaged.

Despite the natural frequency of the modal analysis introducing values of displacements for the model, these deflections must only be utilized to visualize the mode shape. That is, the amounts of the deflections are relative to each other. The natural frequency is a theoretical result due to unspecified dynamic loads, so the results will not depend on displacements. Figure 5 lists the frequencies for the conventional concrete slab for 12 failure modes.

In linear analysis, each single mode shape is separate and independent from other modes. Generally, all mode shapes have different frequencies, with higher modes having higher frequencies, depending on the material type, structure, and the conditions. Figure 6 lists different shapes of modes for the cambered concrete slab.

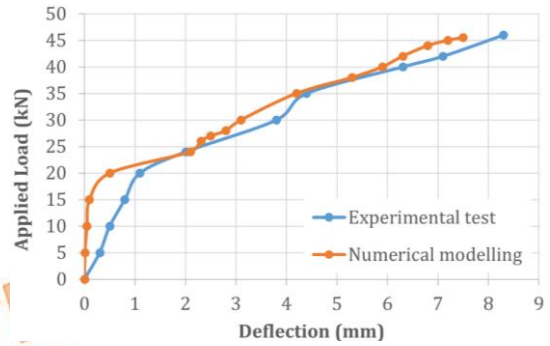

Fig. 4. The experimental versus numerical model validation, the experimental data were taken from [3]

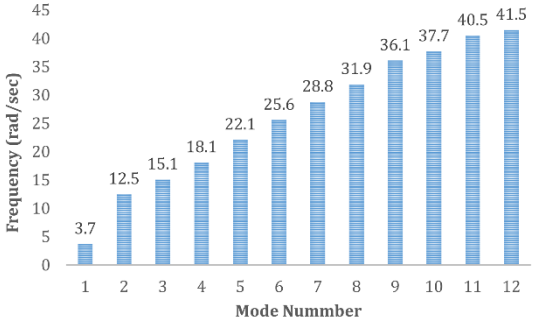

Fig. 5. Model analysis frequencies

5.3. Impulse Load Intensity

After applying different impulse load intensities, the results in Fig. 7 showed that the concrete slab deflects with the loads up and down to enlarge a series of undulations with increasing load amount. All displacement versus time waves fluctuated within the negative range, meaning the slab undergoes nonlinearity. Despite the load becoming zero at 0.03, the concrete slab gave the highest displacement value due to the concentration of the impulse stresses after the hit; then, all curves tend to rest after such a high impact, so the curves fluctuate towards the zero axis. When viewing the nodal displacement of the slab for all loading stages at impulse time (0.02 sec) and at the final period (0.1 sec), it could be noted that the displacement of the concrete slab with the exposing load and the crack patterns. It is clear that the displacement at the exact moment of impulse forms below the loading region and then starts to cross for the remaining parts of the slab due to stress extending.

For low amounts of impulse load, a local failure happens beneath the load. Still, when exposing an impulse larger than the statical failure load, a plastic hinge forms at the side of the slab, which converts it from a fixed slab to a simply supported slab, as shown in Fig. 8 at a load of 60 kN.

5.4. Free Vibration

Two hundred seconds were allowed for the specimens to view the behavior of free vibration waves. Specimens with low intensities of impulse load (4 and 20 kN) introduce waves hesitating between negative and positive axes, which means that the load does not cause any crack in the model till rest after approximately 50 sec and 200 sec for 4kN and 20kN, respectively. While for a slightly higher load (32 kN), the waves showed a sudden large negative displacement at the impulse time (0.2 sec), then started to fluctuate within the negative axis, which means that significant cracks appeared on the model, preventing it from behaving elastically, as illustrated in Fig. 9 and Fig. 10.

When applying loads approximately equal to the static load or higher than it, the model collapses after 0.1 sec, and no wave of free vibration can be obtained (40 kN and 60 kN of load).

A single conclusion can summarize the results: if the impulse load magnitude equals two-thirds of the monotonic failure load or less, the slab still behaves elastically, and no cracks can appear on the model. Still, if the impulse load was higher than or equal to two-thirds of the static load, the model undergoes a plastic deformation. The nodal solution and crack mechanism at the last loading step are provided in Fig. 11.

Steel rebar is also affected by the exposure to load, but for high intensity load. Figure 12 shows the displacement in three directions for the main steel reinforcement due to applying 60 kN of impulse load. This means that there is a specialty for the impulse amount that could change the behavior of reinforced concrete slabs.

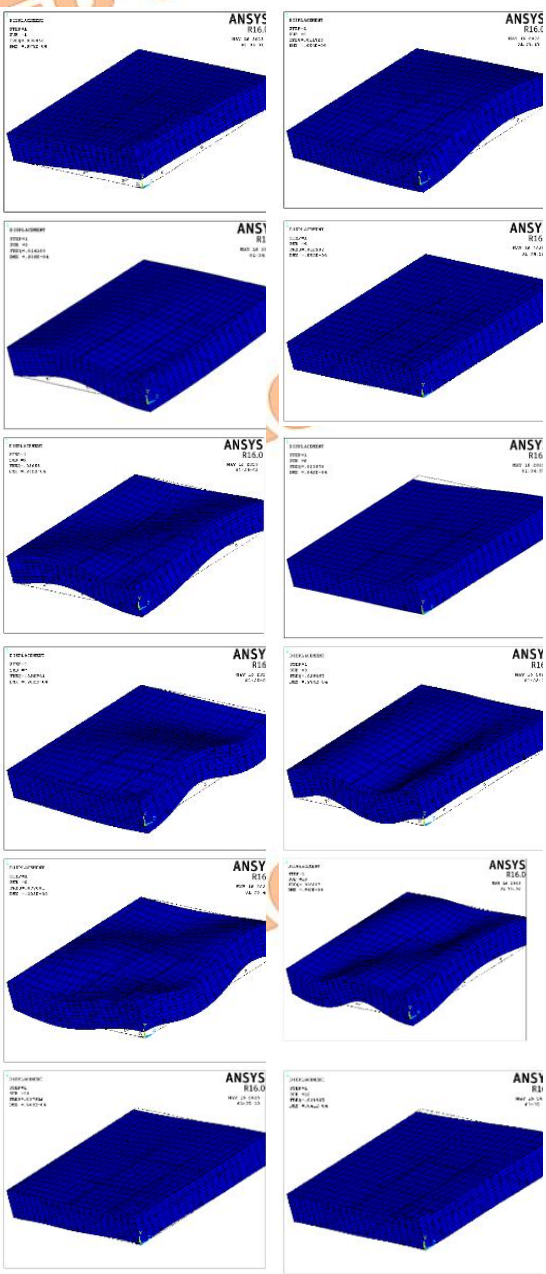

Fig. 6. Several modes of failure for concrete slabs under dynamic loads

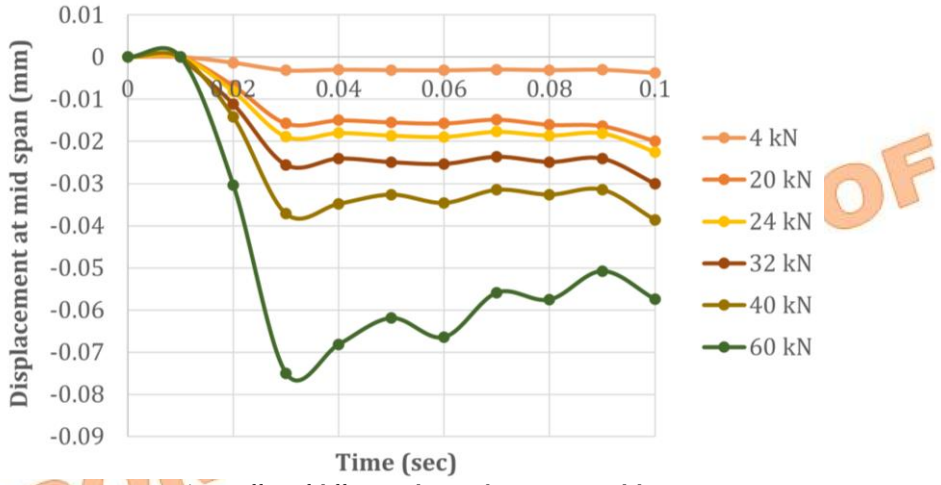

Fig. 7. Effect of different pulses on the concrete model

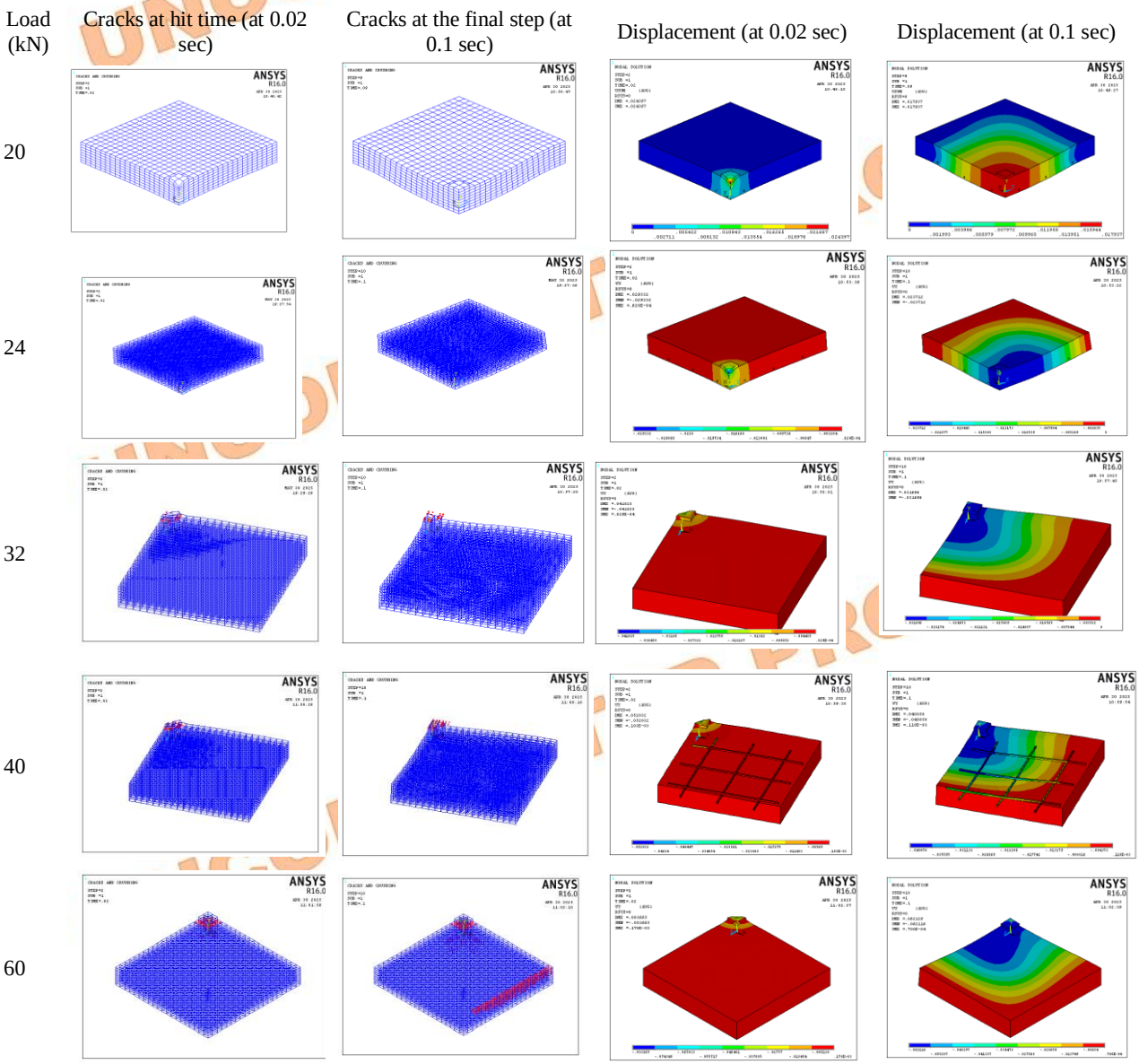

Fig. 8. Crack patterns and nodal displacement for the slab during several impulses and different stages of loadings

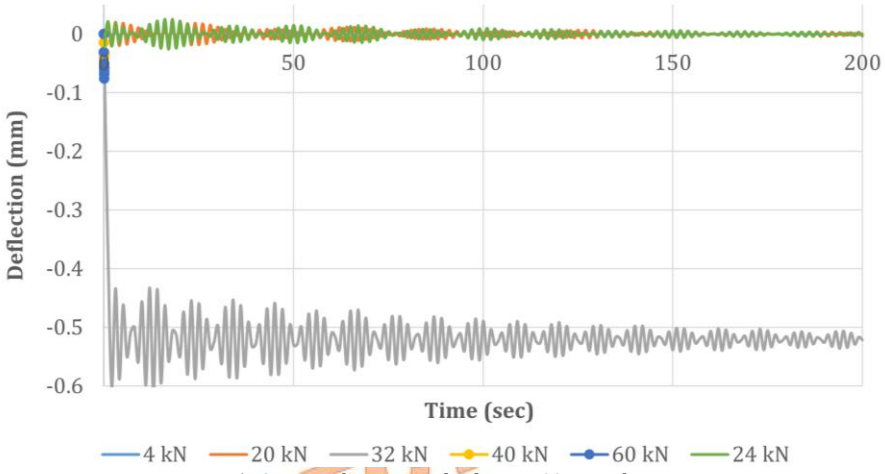

Fig.9. Free vibration results during 200 seconds

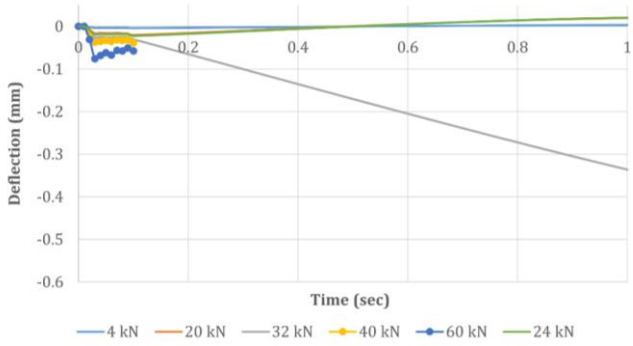

Fig. 10. Clearer curves for the first stage of free vibration

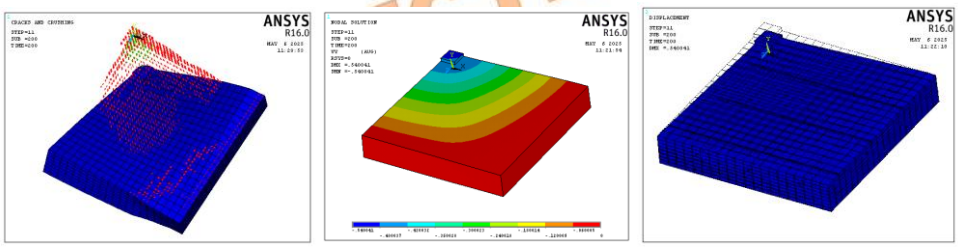

Fig. 11. Crack pattern, nodal displacement, and deformed slab after exposing 32 kN of impulse load

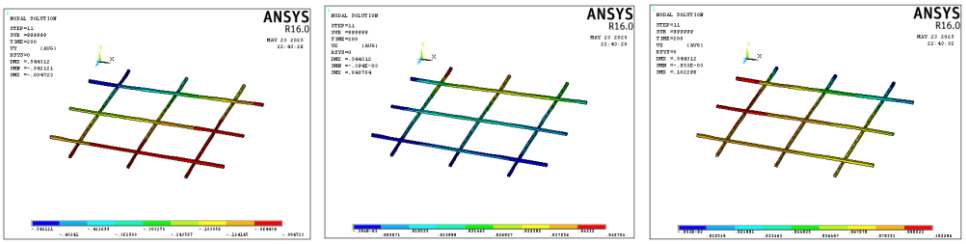

Fig. 12. nodal displacement of steel rebars after 200 sec for Ux, Uy, and Uz

5.5. Influence Of Compressive Strength

The 60kN load intensity model was used to investigate the influence of concrete compressive strength because it presented a critical case. Three different amounts of concrete strength were discussed and inputted with all its accessories, like stress versus strain curves, modulus of elasticity, and the equivalent (8-12% of compressive strength)[19, 20] tensile strength. Results illustrated in Fig. 13 and presented by displacement versus time showed that the deflection of the concrete slab minimized when increasing the concrete strength and keeping the same ripple behavior, i.e., at the same loading steps, the same wave was repeated for all concrete strengths. It can be concluded from such a case that the stronger concrete slab fluctuated similarly but in low deflections due to its strength. The crack paths

leave the supports and recede beneath the applied load after each increment in concrete strength. Nodal displacement participates in the crack pattern with the behavior; the nodal displacement reaches the supports at the weaker concrete slab but recedes towards the applied load after each increment in slab strength, as shown in Fig. 14.

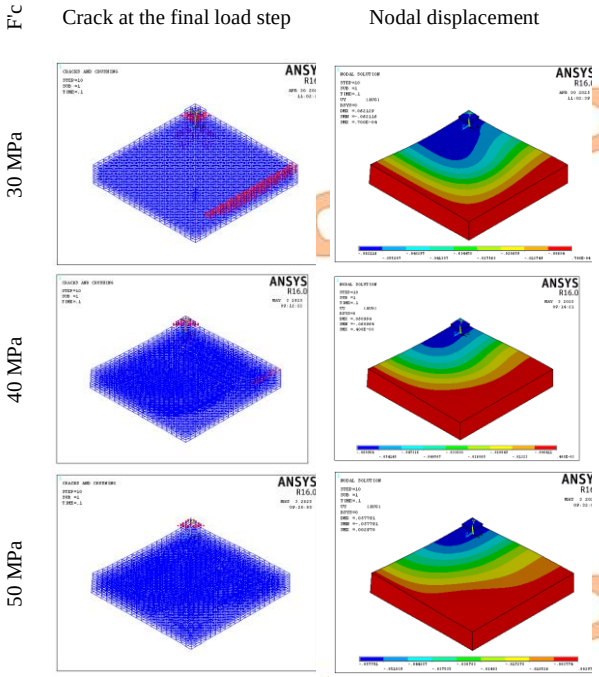

Fig. 14. Nodal solution of the analyzed models

5.6. Rubberized Slab

The 20 kN of load intensity was chosen to investigate the influence of rubcrete mixes. The vibration response of the rubcrete specimens was recorded for 60 sec and provided in Fig. 15. It could be noted that the first point of results after the zero is -0.02 mm, i.e., it started with a negative value due to the impulse, which affected downward. The responses for the models in the first 4 seconds matched each other and then began to behave separately after the 8th second. S30 shows an opposite signal value of deflection when compared with the standard concrete model after the 10th second. The same behavior is observed in S20 at the 11th second. This means that the rubcrete's response to the impulse changed due to energy absorption.

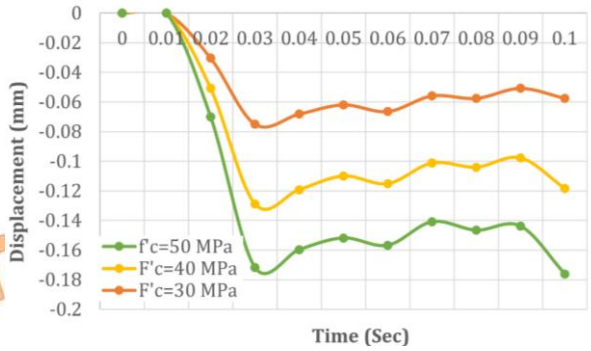

Fig. 13. Influence of concrete compressive strength on the response

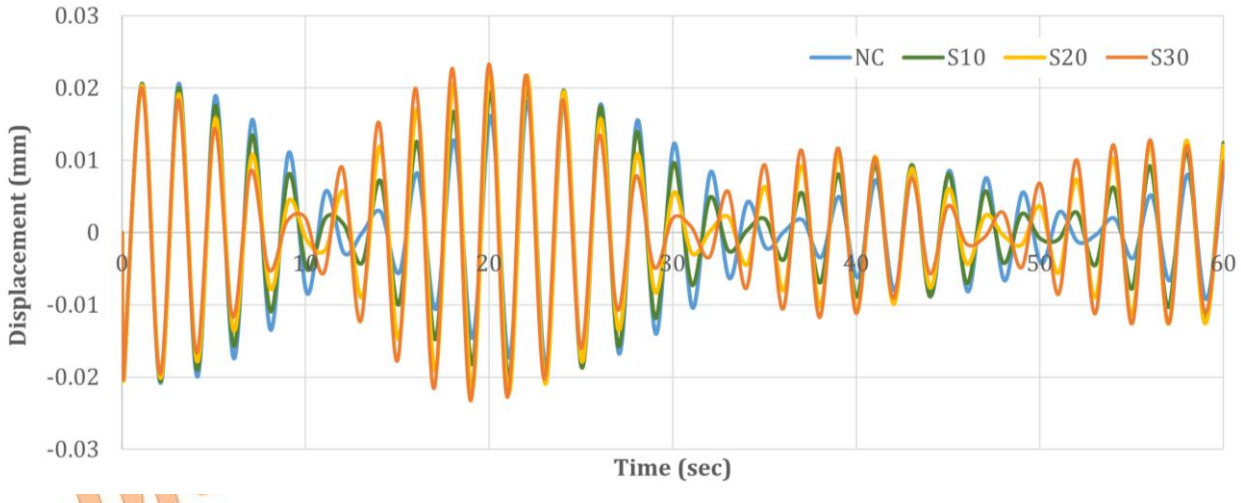

Fig. 15. Changes in wave response due to inserting rubberized concrete properties (with three degrees of replacement) instead of the conventional

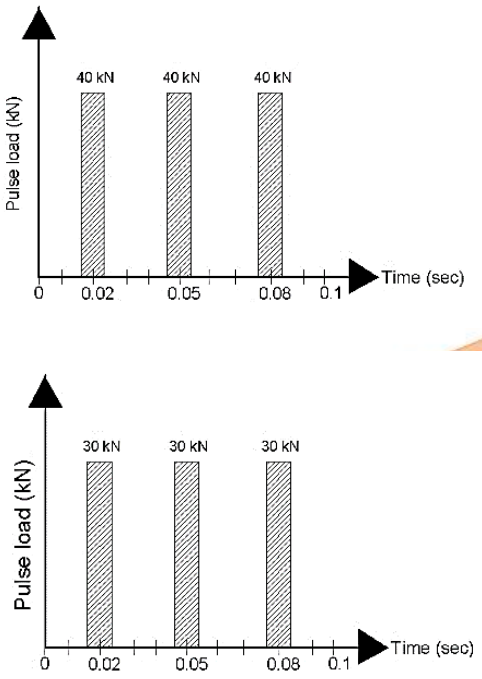

Fig.16. Repeated applied load for 40 and 30 kN, respectively, typically for 20 kN too.

5.7. Influence Of Several Impulses

Repeating load for 3 times for the load intensities equals 20, 30, and 40 kN respectively, and as illustrated in Fig. 16, leads to the conclusion of the time versus displacement curve, which is viewed in Fig. 17. It could be concluded that, repeating the 40 kN load, the concrete slab failed at the second pulse, so that the data of deflection with time was stopped at Fig. 16. The same behavior was observed when repeating 30 kN of load three times. The concrete model overcomes the second hit, but it fails after that, so the results were not continued after 0.06 sec. Exposing 20 kN as a pulse load on the slab three times allows the slab to resist them, but it undergoes plastic deformation and final collapse after 0.1 seconds.

Figure 19 illustrates the final stage of nodal solution before failure by the first and the second hit for 40 kN and 30 kN, respectively.

Figure 20 compares the crack amounts and the width between the second hit and the next second for the 20 kN repeating loads. It could be noticed that the crack increases in quantity and becomes larger after each hit and after the single impulse itself due to stress distribution.

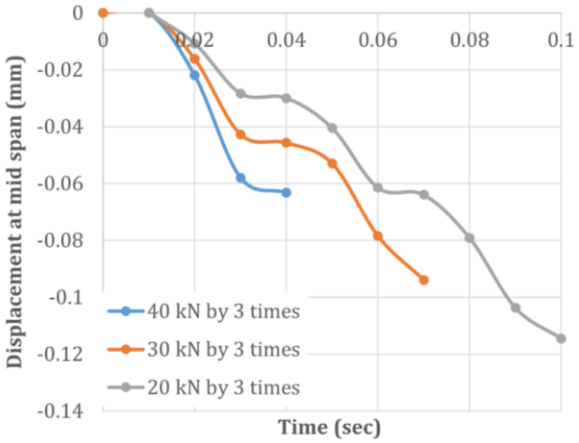

Fig. 17. Concrete slab behavior under repeating impulses

Figure 19 shows a detailed nodal solution for all loading stages, in which it can be concluded that the concrete slab during the impulse does not have much time to undergo all its deformation at the moment of the pulse, so the displacement in the steps next to the hit develops as shown in Fig. 19 at time 0.02 and 0.03 seconds, respectively. The load was exposed at 0.02 sec, and the slab deformed due to it, but when looking at the deformation at 0.03 seconds, the deformation enlarged despite the lack of load at that time. So, it could be said that the concrete slab under impulse load deforms during or even after the applied load due to the high velocity of the applying load.

Furthermore, it is worth mentioning that the concrete slab, after the second hit state to form a plastic hinge at the slab corner, started to be viewed at Fig. 19, time equals 0.06 sec, which indicates that the whole section of the slab resists the applied repeated load, not only the slab center.

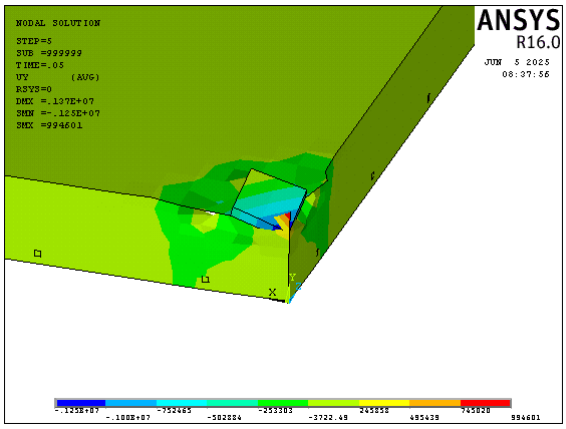

Fig. 18. Model after ending the first hit of 40kN and failure

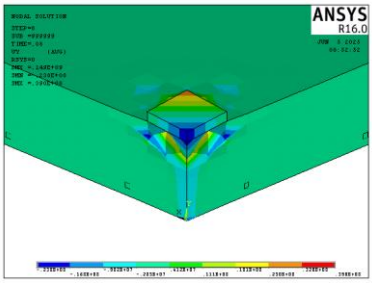

Fig. 19. Model after ending the second hit of 30kN and failure

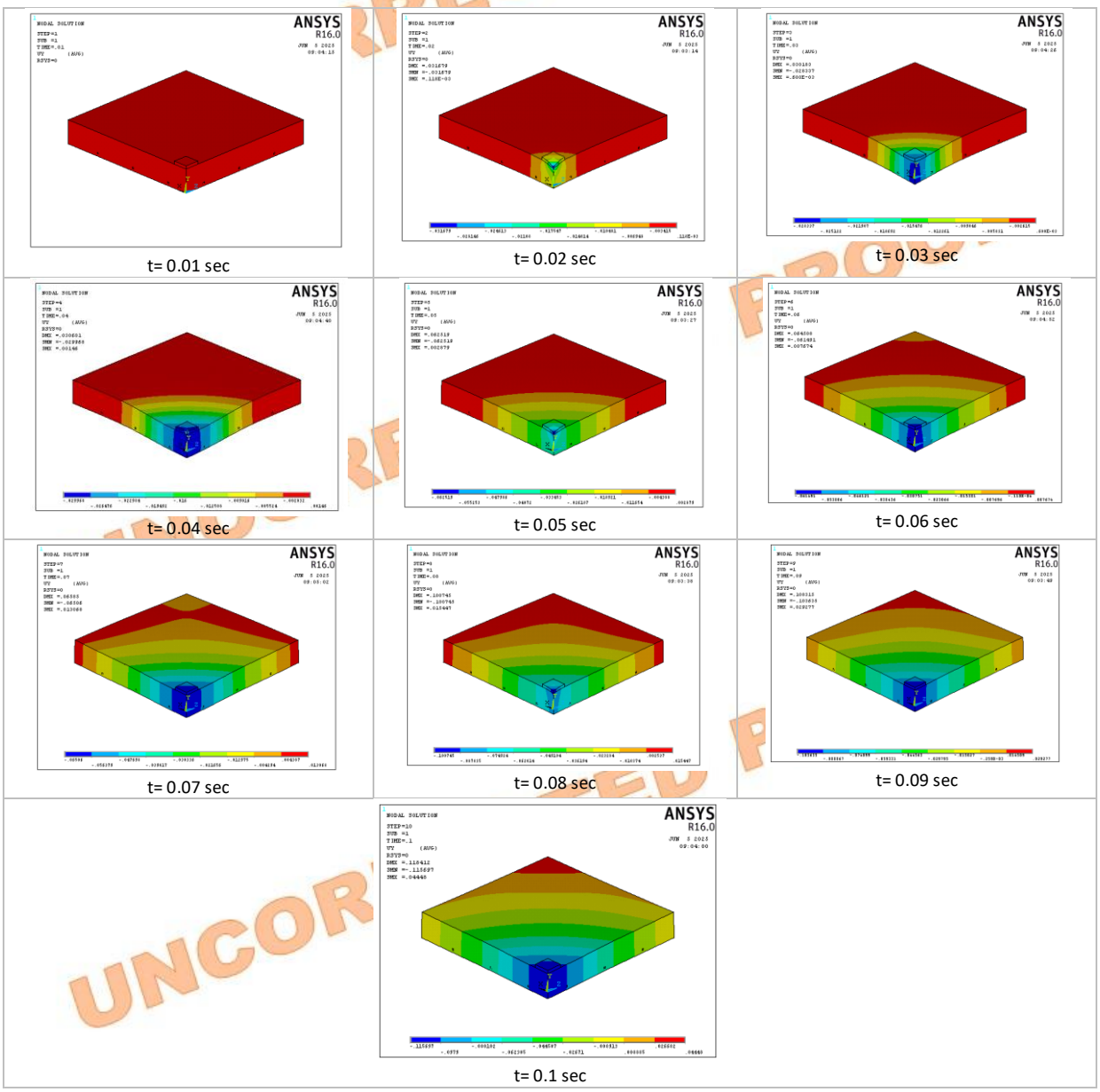

Fig. 20. Nodal solution for all the loading stages of the specimen

6. Conclusions

1. The response of the slab under impulse load depends, to the first degree, on the impulse quantity. If this sudden load equals two-thirds of the static load, the model starts to show visible cracks.
2. It is not conditional on finding the maximum displacement value at the exact second of applying the load, as in the static test; in impulse loading, the designer can expect a higher deflection several seconds after the applied load.
3. Stresses keep spreading after exposing the load till the wave rests.
4. If the response wave rests after the free vibration at the zero deflection, the slab does not undergo nonlinearity. In contrast, when the response rests at a negative deflection value, it could be a notification of plastic cracks happening.
5. The higher concrete compressive strength can change the failure of concrete slabs from global to local failure.
6. The most effective parameter within the rubberized concrete is the modulus of elasticity, which significantly affects the behavior of the rubberized concrete, larger than the stress-strain curve of the rubcrete.
7. Concrete slabs under multi-impulse loads could not overcome the same percentage of pulse, which was identified previously as two-thirds of the monotonic loads. Under repeated pulses, three pulses with a value equal to half of the static loads only, considering the slab will collapse after the third pulse.
8. When comparing several failure modes for multiple impulses, it can be concluded that the crack increases in quantity and becomes larger after each hit and after the single impulse itself due to stress distribution.

References

[1] RayW. Clough and Joseph Penzien, *DYNAMICS OF STRUCTURES*, Second edition. McGraw-Hill Civil Engineering Series, 1993.

[2] H. Hübel, *Simplified Theory of Plastic Zones: Based on Zarka's Method*, First edition. Springer International Publishing, 2017.

[3] S. E. Kadhim and R. F. Makki, 2019. STRUCTURAL BEHAVIOUR OF REACTIVE POWDER REINFORCED CONCRETE SLABS. *Journal of Engineering Science and Technology*. vol. 14, no. 6. pp. 3087–3104, [Online]. Available: https://jestec.taylors.edu.my/Vol 14 issue 6 December 2019/14_6_2.pdf

[4] T. A. Mohammed and H. M. Kadhim, 2022. Static and Dynamic Behavior of High-strength Lightweight Reinforced Concrete One- way Ribbed Slabs. vol. 35, no. 04. pp. 732–739, doi: 10.5829/ije.2022.35.04a.13.

[5] N. Galati, 2007. n-Situ Load Testing: A Theoretical Procedure to Design a Diagnostic Cyclic Load Test on a Reinforced Concrete Two-Way Slab Floor System. *Key Engineering Materials*, doi: 10.4028/www.scientific.net/KEM.347.165.

[6] Ali Sabah Mahdi, Response of Two- way bubble deck reinforced concrete slabs to harmonic load, University of Baghdad/College of Engineering, 2021.

[7] O. M. Makki and H. M. K. Al-Mutairee, 2022. Response of Rubcrete Continuous Deep Beams under Sinusoidal Loads. *International Journal of Engineering*. vol. 35, no. 7. pp. 1184–1191, [Online]. Available: doi: 10.5829/ije.2022.35.07a.10

[8] H. S. Rao, V. G. Ghorpade, N. V. Ramana, and K. Gnaneswar, 2010. Response of SIFCON two-way slabs under impact loading. *International Journal of Impact Engineering*. vol. 37, no. 4. pp. 452–458, [Online]. Available: doi.org/10.1016/j.ijimpeng.2009.06.003

[9] Sunjae Yoo, T.-F. Y. Yoon, HongYoung-Soo, and Y.-S. Yoon, 2020. Damage response of conventionally reinforced two-way spanning concrete slab under eccentric impacting drop weight loading. *Materials*. vol. 13, no. 24, [Online]. Available: https://doi.org/10.1016/j.dt.2022.04.011

[10] Rusinowski.p., Two-way Concrete Slabs with Openings, Lulea University of Technology, Lulea, 2005.

[11] S. M. R. Khalili, M. B. Dehkordi, and M. Shariyat, 2013. Applied Mathematics and Computati on, Modeling, and transient dynamic analysis of pseudoelastic SMA hybrid composite beam. *APPLIED MATHEMATICS AND COMPUTATION*, doi: 10.1016/j.amc.2013.03.092.

[12] M. W. K. and M. F. Ayaho Miyamoto, 1991.

Analysis of Failure Modes for Reinforced Concrete Slabs Under Impulsive Loads. *International Concrete Abstracts Portal, Structural Journal*. vol. 88, no. 5. pp. 538–545, [Online]. Available: doi: 10.14359/2737

[13] M. Muttashar, Effects of impulsive loading and deformation damage on reinforced concrete slabs during building construction. *Periodicals of Engineering and Natural Sciences*. vol. 8, no. 4. pp. 2242–2254, [Online]. Available: doi:10.21533/PEN.V8I4.1715

[14] H. Muteb, G. M. Habeeb, and M. A. Shhatha, Experimental Investigation of Reactive Powder Concrete Slab with Steel Stiffener under Impact Load, 2012.

[15] T. D. H. and F. J. Vecchio, 2014. Behavior of Steel Fiber-Reinforced Concrete Slabs under Impact Load. *Structural Journal*. vol. 111, no. 5. pp. 1213–1224, [Online]. Available: doi: 10.14359/51686923

[16] M. G. Altun and M. Oltulu, 2020. Effect of different types of fiber utilization on the mechanical properties of recycled aggregate concrete containing silica fume. *Journal of Green Building*. vol. 15, no. 1. pp. 119–136, doi: 10.3992/1943-4618.15.1.119.

[17] F. Liu, G. Chen, L. Li, and Y. Guo, 2012. Study of the impact performance of rubber-reinforced concrete. *Construction and Building Materials*. vol. 36. pp. 604–616, doi: 10.1016/j.conbuildmat.2012.06.014.

[18] T. Tahenni, M. Chemrouk, and T. Lecompte, Effect of steel fibers on the shear behavior of high-strength concrete beams, Elsevier, 20AD. [Online]. Available: https://doi.org/10.3389/fmats.2022.1088554

[19] H. Aoude, Structural behaviour of steel fibre reinforced concrete, McGill University, 2007. doi: 10.1680/stco.4.2.57.38230.

[20] O. M. Makki, H. M. K. Almutairee, M. Alibraheemi, and M. M.H., 2024. Experimental Investigation for Sustainable Rubberized Concrete Mixes. *AIP conference proceedings*. vol. 3105, no. 1. pp. 1–10, [Online]. Available: https://doi.org/10.1063/5.0212974

[21] O. M. Makki, 2025. Heat Influence on Sustainable Rubberized Concrete Mixes. *Research on Engineering Structures and Materials (RESM)*. vol. 11, no. 5. pp. 1997–2011.

[22] O. M. Makki, 2026. Strengthened Rubberized Concrete Beams under static and dynamic loads. *International Journal of Engineering*. vol. 39, no. 9. pp. 2075–2088.

[23] E. H. Bani-hani, M. El, H. Assad, M. Al, and Z. Almuqahwi, 2022. Overview of the effect of aggregates from recycled materials on thermal and physical properties of concrete. *Cleaner Materials*. vol. 4, no. March. p. 100087, doi: 10.1016/j.clema.2022.100087.

[24] M. G. H. H. Pritchard, 2015. The yield-line method for concrete slabs: Automated at last. *The Structural Engineer*. vol. 93, no. 10. pp. 44–48, doi: 10.56330/NEDU3095.

[25] P.-K. HSUEH, The Yield-line theory for concrete slabs, B. S., National Taiwan University, 1955.

[26] A. Library Help, 2015. ANSYS Help. *Version 15*.

[27] H. M. Thiyab and H. R. Shaker, 2018. Experimental study of the reinforced concrete continuous beams externally strengthened with carbon fiber reinforced plate. *International Journal of Civil Engineering and Technology*. vol. 9, no. 9. pp. 1766 – 1781, [Online]. Available: https://www.scopus.com/inward/record.uri?eid=2-s2.0-85054732921&partnerID=40&md5=068b5bc600bb6b3dc3173baa091da72d

[28] T. Manual, *Ansys Training Manual Dynamics 7.0*. SAS IP, Inc., 2003. [Online]. Available: https://www.scribd.com/presentation/235698468/Dynamics-70-Toc

[29] E. and G. I. Madenci, *The finite element method and application in civil engineering using ANSYS*. The University of Arizona.

[30] A. Sugianto and S. Taufik, 2019. Numerical Modelling Behaviour of Reinforced Concrete Deep Beam with Strut-and-Tie Model. no. March, doi: 10.5923/j.mechanics.20190901.01.

[31] O. M. Makki and H. M. K. Al-Mutairee, 2022. Mechanical and Dynamical Properties of Structural Rubcrete Mixes.

International Journal of Engineering, Transactions B: Applications. vol. 35, no. 9. pp. 1744 – 1751, doi: 10.5829/ije.2022.35.09C.10.

[32] A. C. I. C. 211, 1991. Standard Practice for Selecting Proportions for Normal, Heavyweight, and Mass Concrete. no. Reapproved.